MedChemComm

RESEARCH ARTICLE

View Article Online
View Journal | View Issue

Check for updates

Cite this: Med. Chem. Commun., 2018, 9, 1733

Antiplasmodial imidazopyridazines: structure–activity relationship studies lead to the identification of analogues with improved solubility and hERG profiles†

Peter Mubanga Cheuka, [a] Nina Lawrence,[b] Dale Taylor,[b] Sergio Wittlin[cd] and Kelly Chibale *[abef]

3,6-Diarylated imidazopyridazines have recently been shown to possess good *in vitro* antiplasmodial and *in vivo* antimalarial activity. However, frontrunner compounds have been associated with poor solubility and a hERG (human *ether-a-go-go*-related gene) inhibition liability raising concerns for potential cardiotoxicity risks. Herein, we report the synthesis and structure–activity relationship studies of new imidazopyridazines aimed at improving aqueous solubility and countering hERG inhibition while maintaining antiplasmodial potency. While we identified new analogues with potent antiplasmodial activity (IC_{50} = 0.031 μM against the NF54 drug-sensitive strain, and IC_{50} = 0.0246 μM against the K1 multidrug resistant strain), hERG inhibition remained an issue. Excitingly, on the other hand, new analogues with a substantially improved hERG inhibition profile (IC_{50} = 7.83–32.3 μM) with sub-micromolar antiplasmodial activity (NF54, IC_{50} = 0.151–0.922 μM) were identified. Similarly, the introduced molecular features also resulted in analogues with moderate to high solubility (60–200 μM) while also displaying sub-micromolar antiplasmodial potency (NF54, IC_{50} = 0.136–0.99 μM).

Received 1st August 2018, Accepted 4th September 2018

DOI: 10.1039/c8md00382c

rsc.li/medchemcomm

Introduction

According to the World Health Organization (WHO) estimates, malaria was responsible for 445 000 deaths and 216 million cases in 2016.[1] The WHO African region accounted for 90% of all malaria cases and 91% of malaria deaths. Children under the age of 5 years are particularly susceptible to infection, illness and death in areas with intense transmission of malaria. Although the under-5 malaria death rate has declined by 29% worldwide, malaria remains a major killer of children in this age group claiming the life of a child every 2 minutes.[1]

Malaria is caused by five species of protozoan parasites of the genus *Plasmodium* which are transmitted to humans through the bites of infected female *Anopheles* mosquitoes.[1] Of the five species known to infect humans, *Plasmodium falciparum* and *Plasmodium vivax* are the most virulent. On the African continent, *P. falciparum* is the most prevalent and causes the most malaria-related deaths worldwide while *P. vivax* dominates most countries outside of sub-Saharan Africa.[1]

Once effective antimalarial drugs like chloroquine and sulfadoxine-pyrimethamine have suffered widespread resistance, which has undermined malaria control efforts.[2–5] Therefore, antimalarial chemotherapy has shifted towards the use of artemisinin combination therapies (ACTs). Regrettably, emerging resistance to artemisinins has been reported recently in 5 countries of the Greater Mekong sub-region, which includes Cambodia, Lao People's Democratic Republic, Myanmar, Thailand and Vietnam.[1] Therefore, with this threat of resistance to first line treatment options, there is a critical need to intensify research efforts into novel, affordable and structurally diverse antimalarials.

Imidazopyridazines possess a range of biological activities including kinase inhibition,[6,7] anxiety treatment[8] and anticancer potential.[9] These compounds have also been

[a] *Department of Chemistry, University of Cape Town, Rondebosch 7701, South Africa. E-mail: Kelly.Chibale@uct.ac.za; Fax: +27 21 6505195; Tel: +27 21 6502553*
[b] *Drug Discovery and Development Centre (H3D), Division of Clinical Pharmacology, Department of Medicine, University of Cape Town, Observatory, Cape Town 7925, South Africa*
[c] *Swiss Tropical and Public Health Institute, Socinstrasse 57, 4002 Basel, Switzerland*
[d] *University of Basel, 4003 Basel, Switzerland*
[e] *Institute of Infectious Disease and Molecular Medicine, University of Cape Town, Rondebosch 7701, South Africa*
[f] *South African Medical Research Council Drug Discovery and Development Research Unit, University of Cape Town, Rondebosch 7701, South Africa*

† Electronic supplementary information (ESI) available: Synthetic and characterization procedures for selected compounds, methods for *in vitro* antiplasmodial evaluation, solubility determination, cytotoxicity evaluation, hERG inhibition and copies of NMR spectra. See DOI: 10.1039/c8md00382c

investigated as potential novel antimalarial agents.[10–13] More recently, 3,6-diarylated imidazopyridazines with potent antiplasmodial activity were identified through a high throughput screening (HTS) of a SoftFocus kinase library.[14] Further medicinal chemistry optimization led to the identification of, among others, the lead compound **1** (Fig. 1) with high *in vitro* potency against both the NF54 (IC_{50} = 7.3 nM) and the K1 (IC_{50} = 6.3 nM) strains of *P. falciparum*.[14] Compound **1** also showed good oral efficacy (98% at 4 × 50 mg kg^{-1}) in the *P. berghei*-infected mouse model.[14] However, the compound exhibited poor solubility (<5 μM at pH 6.5) and a hERG liability (IC_{50} = 0.9 μM). Additionally, the compound only exhibited a mean survival days (MSD) time of 7 days.

In an article published in the same year, Le Manach and colleagues[15] further explored the structure–activity relationship (SAR) of this class of molecules in the hope of addressing the aforementioned shortcomings. Although compound 2 (Fig. 1), identified from this study, completely cured *P. berghei*-infected mice at 4 × 50 mg kg^{-1} per day, better efficacy at lower doses was not achieved. The lead compound also retained sub-optimal solubility (<5 μM at pH 6.5) and some off-target activities such as hERG inhibition. It is noteworthy that this sulfoxide-substituted analogue has no intrinsic hERG potency. But it is rapidly metabolized *in vivo* to the sulfone analogue which has potent hERG activity (IC_{50} = 0.4 μM).[15] In a more recent paper, further expansion of SAR based on modifications to the imidazopyridazine core aimed at improving pharmacokinetics (PK), *in vivo* efficacy and selectivity over hERG were reported.[16] This led to the identification of the pyrazolopyridine analogue in which the two substituents in compound 2 were retained. Despite being able to completely cure *P. berghei*-infected mice at 4 × 50 mg kg^{-1}, the scaffold-hoped analogue still exhibited a hERG liability and poor solubility.[16]

Recently, there has been a significant proportion of drug withdrawals arising from their unwanted prolongation of the time between the start of the *Q* wave and the end of the *T* wave (*QT* interval) in an electrocardiogram.[17] Such a phenomenon, which can lead to malignant ventricular arrhythmia and sometimes sudden cardiac death, is known to arise from, mainly, the blockade of the potassium ion channel (I_{Kr}) encoded by the hERG gene.[17] There are a number of strategies used to address the hERG liability in drug molecules.[18] Herein, we report the application of some of these strategies in designing imidazopyridazine analogues (Fig. 2) with potentially reduced *in vitro* hERG inhibition and improved solubility, which also served to expand the antiplasmodial SAR around this class of molecules. These approaches include subtle modifications (analogues **3–5**, **13** and **28–32**); replacing aromatic rings with saturated systems to discourage π–π stacking with aromatic residues in the large cavity of the hERG channel (analogues **19–21**); introducing polar functionalities into the molecule to potentially disrupt lipophilic drug–hERG interactions (analogues **14–27**).

In a quest to address solubility issues associated with the recently studied antimalarial imidazopyridazines, we employed known strategies, which included introducing polar water-solubilizing groups (analogues **6–12** and **14–27**) and disruption of molecular planarity to discourage the solubility-suppressing effect of π–π stacking (analogues **19–21**).[19–21]

While changes were introduced at positions 3 and 6 of the imidazopyridazine core-scaffold, the 4-methylsulfinylphenyl and 3-methylsulfinylphenyl groups were fixed at these positions in most analogues (analogues **3**, **5–8**, and **10–27**). Le Manach and co-workers have recently employed such a prodrug strategy by synthesizing solubility-enhancing sulfoxides which were shown to be metabolized *in vivo* to the corresponding active sulfones.[15] In two cases, sulfone-containing derivatives, **4** and **9**, were also synthesized for comparison purposes. For derivatives bearing sulfoxide-containing phenyl rings at the point of variation, sulfone counterparts were synthesized for the same reason in some cases (*e.g.*, analogues **3** *vs.* **5**, **14** *vs.* **15**, **16** *vs.* **17**, **24** *vs.* **27**, and **25** *vs.* **26**).

Results and discussion

Chemistry

Analogues **1**, **4–12**, **14–23** and **29–32** were synthesized according to Scheme 1. The intermediate **2a** was obtained by condensation/cyclization of commercially available 6-chloropyridazin-3-amine (**1a**) with bromoacetaldehyde diethylacetal in the presence of hydrobromic acid (HBr).[14] A regioselective electrophilic aromatic iodination using *N*-iodosuccinimide (NIS) afforded the iodinated intermediate, **3a**, in 81% yield.[14] Sequential Suzuki–Miyaura cross coupling reactions on intermediate **3a** delivered the diaryl-imidazopyridazines (**1**, **4–12** and **29–32**) in 13–80% yield.[14] The aminated target molecules, **14–23**, were realized, in poor to low yields (8–30%), *via* a palladium-mediated Buchwald–Hartwig amination[22,23] of the chloro-bearing intermediate **4a**. The aniline starting materials **5d** and **5h**, which were used to synthesize analogues **22** and **23** respectively, were not available commercially. These were synthesized in-house according to the synthetic schemes in the ESI.†

Scheme 2A and B were used to synthesize analogues **3**, **13**, **24–27** and **28**. Using an excess (2.2 equivalents) of the respective boronic acid, analogues **3** and **28** were obtained by a one

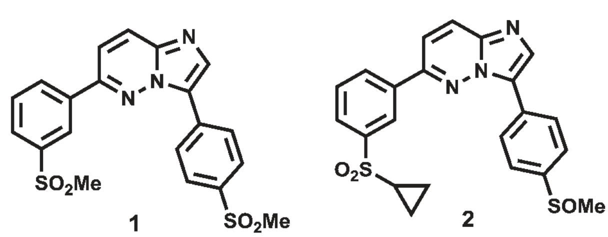

1 **2**

P. f, NF54 IC_{50} = 7.3 nM
P. f, K1 IC_{50} = 6.3 nM
In vivo P. berghei (po) at 4 × 50 mg/kg, 98%, 7 MSD
hERG IC_{50} = 0.9 μM

P. f, NF54 IC_{50} = 1.1 nM
In vivo P. berghei (po) at 4 × 50 mg/kg, 99.8%, > 30 MSD, 3 out of 3 mice cured

Fig. 1 Previously explored antimalarial imidazopyridazine analogues.

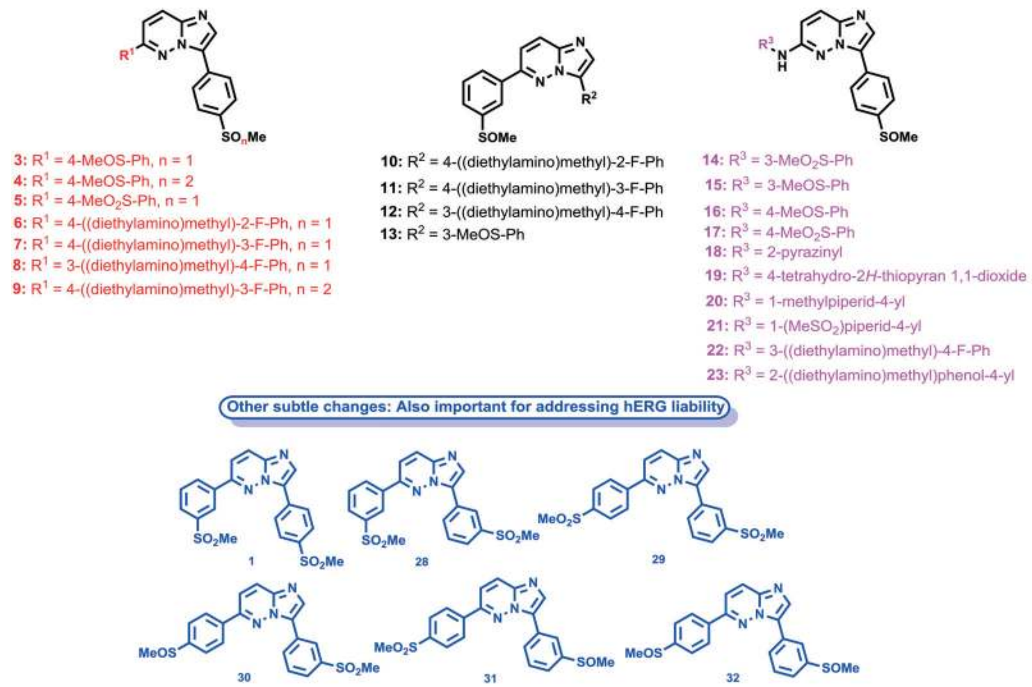

Fig. 2 Structural modifications made around the imidazopyridazine core.

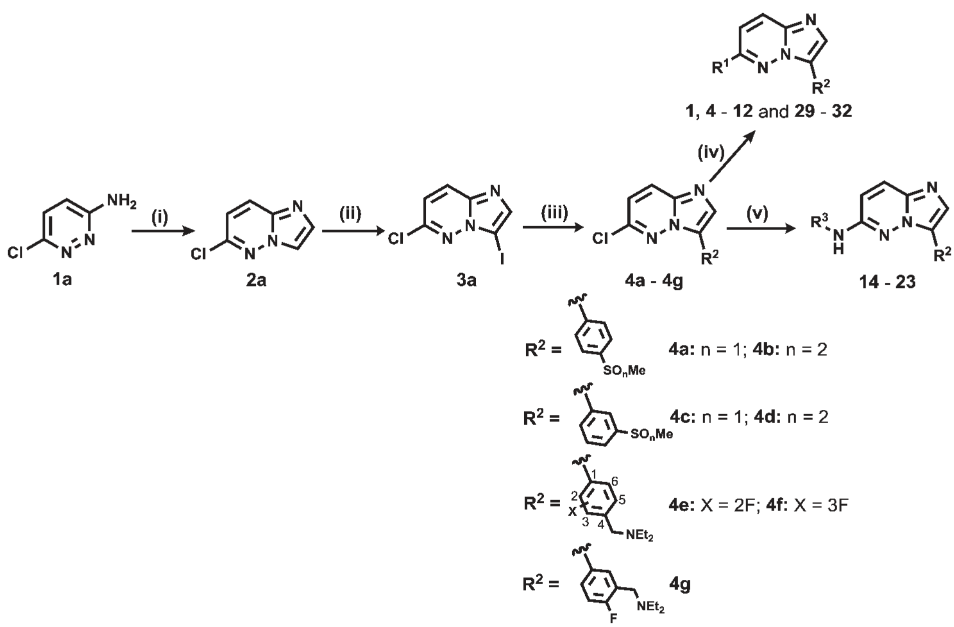

Scheme 1 General synthetic approach for analogues **1**, **4–12**, **14–23** and **29–32**. Reagents and conditions: (i) $BrCH_2CH(OEt)_2$, aq HBr, EtOH/H_2O, reflux, 103 °C, 22 h; (ii) NIS, DMF, rt (21 °C), 5 d, 81%; (iii) appropriate boronic acid or boronic acid pinacol ester, $Pd(PPh_3)_2Cl_2$, 1 M aq K_2CO_3, DMF, 80 °C, 3.5–46 h, 26–77%; (iv) appropriate boronic acid or boronic acid pinacol ester, $Pd(PPh_3)_2Cl_2$, 1 M aq K_2CO_3, DMF, 100 °C, 4–21 h, 13–80%; (v) R_3NH_2, $Pd_2(dba)_3$, (*R*)-BINAP for **17**, BrettPhos for **14**, **22** & **23**, XPhos for **15**, **16** & **18–21**, K_2CO_3 for **17**, Cs_2CO_3 for **14**, **22** & **23**, NaO*t*-Bu for **15**, **16** & **18–21**, toluene/1,4-dioxane for **17**, 1,4-dioxane for all other analogues, 100 °C for **20**, 120 °C for all other analogues, sealed tube, inert atmosphere (N_2), 6–43 h, 8–30%.

pot Suzuki–Miyaura cross-coupling on both reaction sites of the previously synthesized intermediate **3a** (Scheme 2A).[14] Analogues **13** and **24–27** were obtained *via* a common bromo-substituted intermediate **4i** according to Scheme 2B. Intermediate **4i** was synthesized from a previously synthesized imidazopyridazine intermediate **2a** by a Suzuki–Miyaura cross coupling followed by regioselective electrophilic aromatic substitution in presence of *N*-bromosuccinimide (NBS).[14] A Suzuki–Miyaura cross-coupling on intermediate **4i** furnished analogue **13** in 40% yield. The aminated derivatives **24–27**

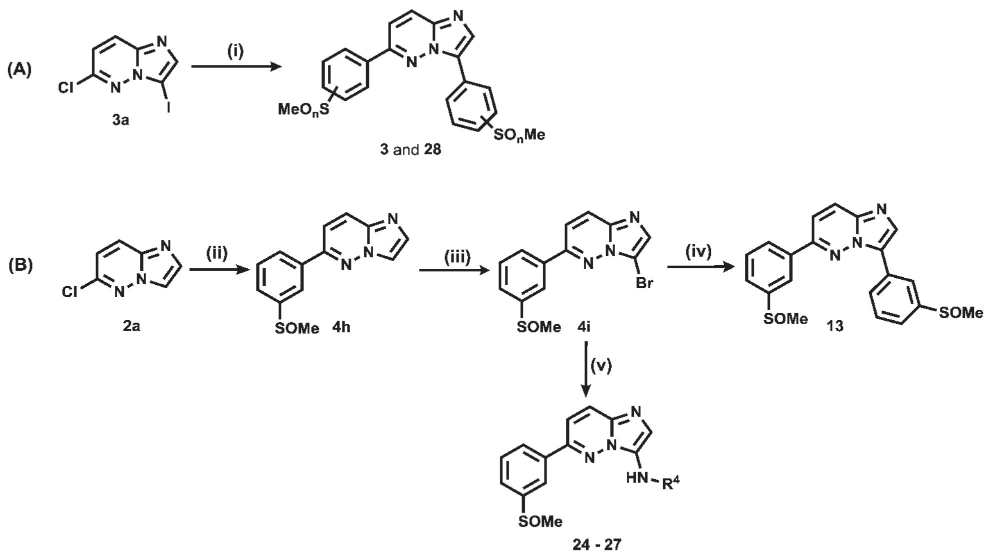

Scheme 2 General synthetic approach for analogues **3**, **13**, **28** and **24–27**. Reagents and conditions: (i) appropriate boronic acid (excess, 2.2 eq.), $Pd(PPh_3)_2Cl_2$, 1 M aq K_2CO_3, DMF, 100 °C, 15 h for **3** and 24 h for **28**, 39% for **3** and 62% for **28**; (ii) 3-methylsulfinylphenylboronic acid, $Pd(PPh_3)_2Cl_2$, 1 M aq K_2CO_3, DMF, 100 °C, 3.25 h, 48%; (iii) NBS, DMF, rt (23 °C), 22 h, 59%; (iv) 3-methylsulfinylphenylboronic acid, $Pd(PPh_3)_2Cl_2$, 1 M aq K_2CO_3, DMF, 100 °C, 20 h, 40%; (v) R_4-NH_2, $Pd_2(dba)_3$, BrettPhos, Cs_2CO_3, 1,4-dioxane, 120 °C, sealed tube, 5–39 h, 9–17%.

were obtained in poor yields (9–17%) *via* Buchwald–Hartwig amination.[22,23]

Biology and solubility

A total of 31 imidazopyridazine analogues were synthesized and tested in biological and solubility assays. All the synthesized analogues were evaluated for *in vitro* antiplasmodial activity against the drug sensitive strain (NF54) of the *P. falciparum* malaria parasites. Analogues exhibiting submicromolar ($IC_{50} < 1$ μM) potency were further tested *in vitro* against the multi drug-resistant strain (K1) of *P. falciparum*. In parallel, the solubility of all the synthesized analogues was determined. Significantly potent ($IC_{50} < 1$ μM) analogues were advanced to cytotoxicity testing using the Chinese Hamster Ovary (CHO) cell line (ATCC). The selectivity index (SI) for each compound was calculated as a ratio of cytotoxic IC_{50} value to corresponding antiplasmodial (*P. f* NF54) IC_{50} value. The SAR explorations are discussed with reference to IC_{50} values on the NF54 strain. Representative compounds were selected and screened for hERG activity on the QPatch gigaseal automated patch clamp platform.

***In vitro* antiplasmodial activity and solubility.** The *in vitro* antiplasmodial (IC_{50} values), and solubility values for all the synthesized compounds are shown in Tables 1–3.

We set out by fixing a 4-methylsulfinylphenyl group at position 3 while introducing saturation, subtle modifications and water-solubilizing groups at position 6 (Table 1). The antiplasmodial potency of all analogues in this series was generally compromised (IC_{50} = 0.136–2.67 μM) compared to the previously reported[14] lead compound **1** (IC_{50} = 0.0034 μM). All analogues evaluated for antiplasmodial activity against both the NF54 and K1 parasites were equipotent on these two strains, suggesting the absence of cross-resistance. This is in conformity with previously reported imidazopyridazine derivatives.[15] *Para* substitution with either a sulfone or sulfoxide group at 6-phenyl ring proved detrimental to potency as reflected in analogues **3** (IC_{50} = 0.673 μM) and **5** (IC_{50} = 0.974 μM). As anticipated, the sulfoxide-substituted analogue **3** exhibited superior solubility (200 μM) compared to the sulfone-substituted analogue **5** (5 μM). Amongst the analogues substituted with a fluoro and a basic side chain (**6**, **7** and **8**, Table 1), **8** proved the most potent (IC_{50} = 0.136 μM) signifying the importance of the *para*-fluoro and *meta*-diethylaminomethyl substitution pattern to potency. It is noteworthy that compound **8** was also the most potent in the entire series of analogues in Table 1. Gratifyingly, we also managed to significantly improve solubility in such basic amine-substituted analogues (180–200 μM). Although potency was, generally, compromised for the aminated imidazopyridazines, most of them still retained sub-micromolar potency. Notable amongst these is 3-methylsulfonylaniline-substituted analogue **14** (IC_{50} = 0.274 μM) which was 3-fold more potent than the reduced form **15** (IC_{50} = 0.820 μM). However, the *para*-substituted versions **16** (IC_{50} = 0.552 μM) and **17** (IC_{50} = 0.423 μM) were equipotent. In this series, we also designed analogues with saturated cyclic groups (**19–21**) which we hypothesized could help discourage π–π stacking thereby improving aqueous solubility.[24] Strikingly, the sulfone group in analogue **21** (IC_{50} = 0.498 μM) was important in retaining sub-micromolar potency – analogue **20** lacking this group exhibited 5-fold less potency (IC_{50} = 2.67 μM). All the aminated analogues, generally exhibited improved solubility with sulfone-substituted analogues showing inferior solubility relative to their sulfoxide counterparts.

Table 1 *In vitro* antiplasmodial activity against *P. falciparum* (NF54 and K1) and solubility of pyridazine-substituted analogues

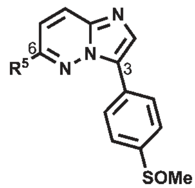

Compound code	R^5	*P. f* IC_{50},[a,b] μM NF54	*P. f* IC_{50},[a,b] μM K1	Solubility, μM, pH 6.5
3	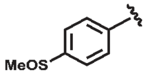	0.673	0.499	200
5	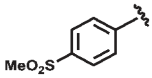	0.974	0.82	5
6	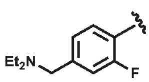	1.88	ND[c]	180
7	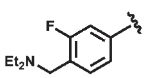	1.67	ND[c]	195
8	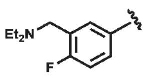	0.136	0.114	200
22	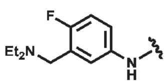	1.62	ND[c]	200
23	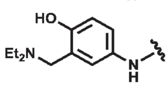	0.922	0.774	195
14	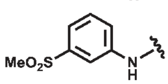	0.274	0.236	20
15	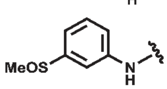	0.820	0.854	190
16	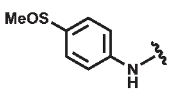	0.552	0.488	195
17	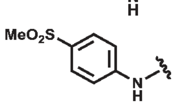	0.423	0.236	<5
18	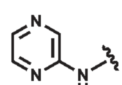	0.468	0.436	25
19	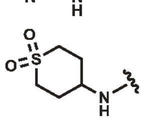	0.524	0.492	10
20	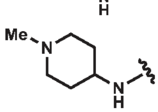	2.67	ND[c]	200
21	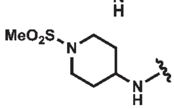	0.498	0.439	70

[a] Mean from *n* values of ≥2 independent experiments with multidrug resistant (K1) and sensitive (NF54) strains of *P. falciparum*. The majority of the individual values differed less than 2-fold (maximum 2-fold). [b] Artesunate [IC_{50} = 2.2 ng mL^{-1} (NF54), 0.93 ng mL^{-1} (K1)] and chloroquine [IC_{50} = 4.3 ng mL^{-1} (NF54), 83 ng mL^{-1} (K1)] were used as reference drugs. [c] ND, not determined.

Inspired by previous studies[14] which found *meta*-substitution at the phenyl ring on position 6 optimal for potency, we kept this group fixed as 3-methylsulfinylphenyl group while exploring other changes at position 3 of the core-scaffold. The antiplasmodial and solubility results are shown in Table 2. Apart from compound **13**, which exhibited promising activity against both the NF54 (IC_{50} = 0.151 μM) and K1 (IC_{50} = 0.0866 μM) strains, generally, this series represented modifications which compromised potency the most (IC_{50} = 0.99–7.55 μM). However, the introduced water-solubilizing groups imparted moderate to high solubility (35–200 μM) in these analogues. An increase in dihedral angle which compromises π–π stacking following *ortho* substitution of bi-aryl systems could explain the notable difference in solubility between the *ortho*-fluorinated analogue **10** (200 μM) and the *meta*-fluorinated regioisomer **11** (35 μM).[24] As previously observed, sulfoxide-containing aminated analogues **26** (150 μM) and **27** (165 μM) were more soluble than the corresponding sulfone analogues **25** (40 μM) and **24** (60 μM).

In another strategy to address the hERG liability, we designed analogues **4**, **28–32** (Table 3), **3**, **5** and **13** (Table 1) with subtle modifications, a strategy that has also been used by other drug discovery programmes to diminish hERG activity.[18] These included peripheral positional changes of the sulfone and sulfoxide groups on the two phenyl rings as well as switching sulfones with sulfoxide groups. The sulfone version of compound **7** in Table 1, compound **9** (Table 3), was also included in this series of compounds. Interestingly, compound **28**, a regioisomer of the previously reported[14] lead compound **1** was highly potent (IC_{50} = 0.031 μM) indicating that the *para*-to-*meta* positional change of the right-hand-side sulfone was tolerated albeit solubility (<5 μM) was still an issue. However, this isomer is still 9-fold less potent than the lead compound **1** (IC_{50} = 0.0034 μM) indicating a slight decrease in potency accompanies this positional change. While maintaining the sulfone at the *meta* position on the right-hand-side phenyl ring, *para* substitution on the left-hand-side phenyl ring, irrespective of the nature of substituent as shown in analogues **29** (IC_{50} = 0.396 μM) and **30** (IC_{50} = 0.264 μM) was detrimental to potency. Similarly, keeping the sulfoxide fixed at the *meta* position of the right-hand-side phenyl ring while introducing the sulfone and sulfoxide groups at the *para* position of the left-hand-side phenyl ring proved detrimental to potency (see analogues **31**, IC_{50} = 1.68 μM and **32**, IC_{50} = 0.870 μM). It is also noteworthy that the sulfoxide-substituted analogue **32** was twice as potent as the sulfone-substituted counterpart **31**. Furthermore, analogue **4** was 7-fold less potent than its previously reported[15] regioisomer further confirming that *para*-substitution on the left-hand-side phenyl ring is detrimental to activity. Save for analogue **9**, whose excellent solubility (200 μM) could be attributed to the water-solubilizing basic side chain, all analogues in this series having at least one sulfone group were poorly soluble (<5–10 μM). As expected, analogue **32** with

Table 2 *In vitro* antiplasmodial activity against *P. falciparum* (NF54 and K1) and solubility of imidazo-substituted analogues

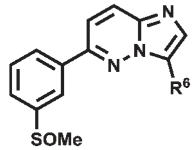

Compound code	R^6	*P. f* IC_{50},^{a,b} μM NF54	K1	Solubility, μM, pH 6.5
10	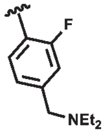	3.2	ND[c]	200
11	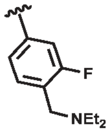	1.05	ND[c]	35
12	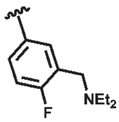	0.99	0.558	200
13	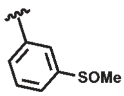	0.151	0.0866	200
24	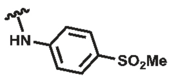	3.62	ND[c]	60
25	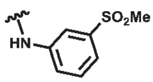	7.55	ND[c]	40
26	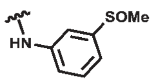	4.71	ND[c]	150
27	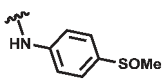	3.81	ND[c]	165

[a] Mean from *n* values of ≥2 independent experiments with multidrug resistant (K1) and sensitive (NF54) strains of *P. falciparum*. The majority of the individual values differed less than 2-fold (maximum 2-fold). [b] Artesunate [IC_{50} = 2.2 ng mL^{-1} (NF54), 0.93 ng mL^{-1} (K1)] and chloroquine [IC_{50} = 4.3 ng mL^{-1} (NF54), 83 ng mL^{-1} (K1)] were used as reference drugs. [c] ND, not determined.

sulfoxide-substituted phenyl rings, exhibited excellent solubility (200 μM).

In vitro **mammalian cytotoxicity and hERG inhibition.** Analogues with *in vitro* antiplasmodial potency IC_{50} < 1 μM were evaluated for *in vitro* cytotoxicity against the mammalian CHO cell line. Analogues screened for hERG inhibition were, generally, selected based on demonstrated sub-micromolar antiplasmodial activity. However, for derivatives representing discreet peripheral changes (*e.g.*, **3–5**, **13**, **28–30** and **32**) with sub-micromolar antiplasmodial activity, only representative compounds were tested for hERG inhibition. Generally, most analogues were non-cytotoxic with selectivity indices in the range 72–>874 (Table 4). Strikingly, compounds **8**, **9**, **12** and **23**, containing the basic side chains, were particularly cytotoxic with lower selectivity (SI = 10–30) (Table 4).

The hERG inhibition results for selected analogues are summarized in Table 4. As previously reported,[14] compound **1** was potent on hERG (IC_{50} = 3.61 μM). Its isomers, **28** (IC_{50} = 2.35 μM) and **29** (IC_{50} = 4.0 μM), still retained hERG potency. When sulfones in compound **28** were switched to sulfoxides as shown in compound **13** (IC_{50} = 8.45 μM), hERG potency was found to diminish by almost 4-fold. Moreover, positional change of the left-hand-side sulfoxide group in **13** to *para* in analogue **32** (IC_{50} = 21.1 μM) significantly lowers hERG activity. When compared to the lead compound **1**, *para* sulfoxide substitution on the left-hand-side phenyl ring, as shown in analogue **4** (IC_{50} = 17.9 μM), reduced hERG potency by 5-fold. Analogues with basic side chains, **8** (IC_{50} = 0.59 μM), **9** (IC_{50} = 5.2 μM) and **23** (IC_{50} = 7.83 μM) were potent on the hERG channel. This is not unexpected since most

Table 3 *In vitro* antiplasmodial activity against *P. falciparum* (NF54 and K1) and solubility for discreetly-modified analogues

Compound code	Structure	*P. f* IC_{50},[a,b] μM		Solubility, μM, pH 6.5
		NF54	K1	
4	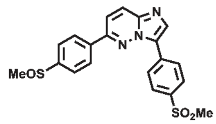	0.278	0.207	10
9	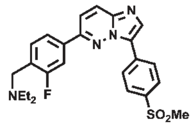	0.822	ND[c]	200
1	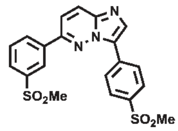	0.0034	0.00225	10
28	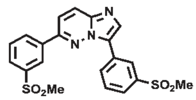	0.031	0.0246	<5
29	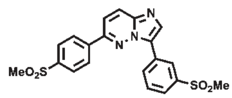	0.396	0.314	<5
30	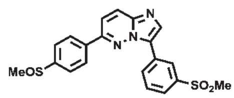	0.264	0.189	<5
31	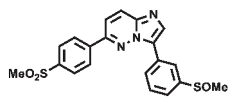	1.68	ND[c]	<5
32	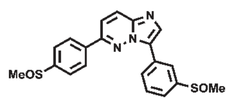	0.870	0.872	200

[a] Mean from *n* values of ≥2 independent experiments with multidrug resistant (K1) and sensitive (NF54) strains of *P. falciparum*. The majority of the individual values differed less than 2-fold (maximum 2-fold). [b] Artesunate [IC_{50} = 2.2 ng mL^{-1} (NF54), 0.93 ng mL^{-1} (K1)] and chloroquine [IC_{50} = 4.3 ng mL^{-1} (NF54), 83 ng mL^{-1} (K1)] were used as reference drugs. [c] ND, not determined.

ligands that block the hERG channel contain a basic nitrogen,[18] which can get protonated at physiological pH thereby facilitating hERG binding through cation–π interactions between the protonated nitrogen and the π system of the aromatic residues in the channel cavity.[18] For the aniline derivatives, **14–17**, *meta* sulfonylation seems to enhance hERG activity (**14**, IC_{50} = 2.36 μM). Strikingly, switching the sulfone in **14** with the sulfoxide diminishes hERG activity by about 8-fold as demonstrated in analogue **15** (IC_{50} = 18.2 μM). The regioisomer of **15**, compound **16** (IC_{50} = 32.3 μM), which is *para* substituted showed further decrease in hERG inhibition. Interestingly, a positional change from *meta* to *para* (**14** to **17**) also led to a 11-fold reduction in hERG activity. We also hypothesized that the introduced saturated rings in **19** and **21** would reduce hERG binding by disrupting π–π interactions between phenyl rings in our molecules and those embedded in the channel cavity.[18] Interestingly, both analogues **19** (IC_{50} = 28.8 μM) and **21** (IC_{50} = 25.9 μM) indeed displayed significantly weaker hERG inhibition activity.

Conclusion

In our efforts to improve solubility and counter hERG inhibition, we identified a regioisomer of lead **1**, compound **28** (Tables 3 and 4) with potent *in vitro* antiplasmodial activity (IC_{50} = 0.031 μM) and high selectivity (SI = 377) against the CHO cell line. However, hERG inhibition (IC_{50} = 2.35 μM) and poor solubility (<5 μM) remain issues. Interestingly, the sulfoxide version, compound **13** (Tables 2 and 4), exhibited excellent solubility (200 μM) with reduced hERG inhibition (IC_{50} = 8.45 μM). Additionally, we successfully managed to substantially reduce hERG activity in molecules **4**, **13**, **15–19**, **21**, **23** and **32** (IC_{50} = 7.83–32.3 μM, Table 4). Similarly, the introduced molecular features also resulted in analogues **3**, **6–10**,

Table 4 *In vitro* mammalian cytotoxicity and hERG inhibition profiling for selected analogues

Compound code	Structure	Cytotoxicity[b] CHO cells IC$_{50}$, μM (SD)	Cytotoxicity[b] CHO cells SI[c]	hERG IC$_{50}$, μM (SD)[d]
1	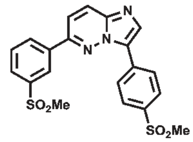	>234	>69 000	3.61 (0.623)
28	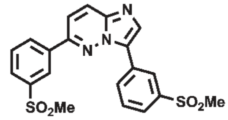	11.7 (0.89)	377	2.35 (0.46)
13	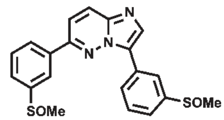	31.1 (0.2)	206	8.45 (0.8)
29	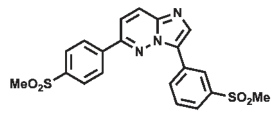	181 (5.2)	457	4 (0.83)
30	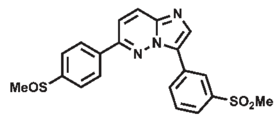	18.9 (1.5)	72	ND[a]
32	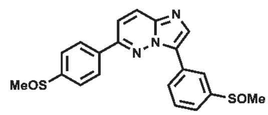	106 (21)	122	21.1 (2.8)
3	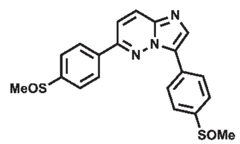	>253	>376	ND[a]
5	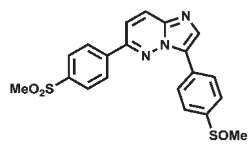	>243	>249	ND[a]
4	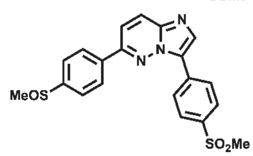	>243	>874	17.9 (5.56)
8	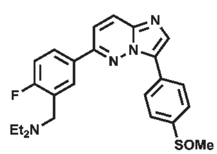	4.08 (0.96)	30	0.59 (0.02)
23	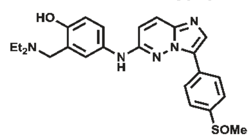	9.41 (3.0)	10	7.83 (1.21)
14	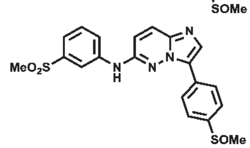	123 (0.4)	449	2.36 (0.21)

Table 4 *(continued)*

Compound code	Structure	Cytotoxicity[b] CHO cells		hERG IC_{50}, μM (SD)[d]
		IC_{50}, μM (SD)	SI[c]	
15	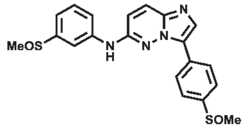	ND[a]	ND[a]	18.2 (8.45)
16	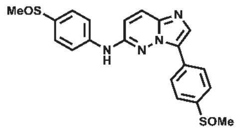	>244	>442	32.3 (1.54)
17	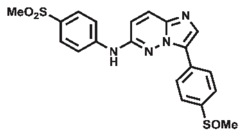	>234	>553	26.1 (6.30)
18	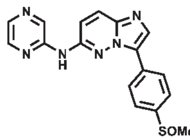	277 (18)	592	7.84 (0.76)
21	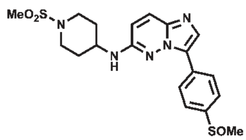	>231	>464	25.9 (1.83)
19	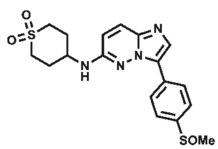	>247	>471	28.8 (3.64)
9	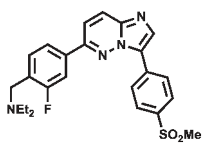	9.44 (2.1)	11	5.2 (0.44)
12	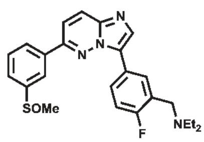	12 (2.7)	12	ND[a]

[a] ND, not determined. [b] Mean from n = 3 independent experiments; SD, standard deviation; emetine was used as a reference drug (IC_{50} = 0.033 ± 0.006 μM). [c] SI = selectivity index = IC_{50} (CHO)/IC_{50} (*P. f* NF54). [d] Mean from n = 3 independent experiments; verapamil was used as a positive control (IC_{50} = 0.560 ± 0.0961 μM).

12, 13, 15, 16, 20–24, 26, 27 and **32** (Tables 1–3) with moderate to high solubility (60–200 μM).

Experimental procedures

Chemistry

All reagents and chemicals used in all reactions were purchased from various commercial sources and used without further purification. All the solvents used in the reactions were anhydrous save for ethanol which was absolute (99.9%). Reactions were monitored by a combination of analytical thin layer chromatography (TLC) and liquid chromatography mass spectrometry (LC-MS). The TLC plates were sourced from Merck (TLC Silica gel 60 F_{254} aluminium-backed) and were developed in a 100 mL beaker covered with either a watch glass or aluminium foil. The plates were visualized under ultraviolet light (UV 254 and 366 nm). An Agilent LC-MS instrument with the following components was used for compound purity checks and reaction monitoring: Agilent 1260® Infinity Binary Pump, Agilent 1260® Infinity Diode Array Detector, Agilent 1290® Infinity Column Compartment, Agilent 1260® Infinity Autosampler, Agilent 6120® Quadrupole LC-MS, and Peak Scientific® Genius 1050 Nitrogen Generator. An X-Bridge® (C18, 2.5 μm, 3.0 mm (ID) × 50 mm length) column maintained at 35 °C or 40 °C was used. The chromatographic mobile phase was composed of 10 mM aqueous ammonium acetate (NH_4Ac) spiked with 0.4% acetic acid while the organic phase was composed of 10 mM NH_4Ac in methanol spiked with 0.4% acetic acid. The mass spectra were acquired using electrospray ionisation (ESI) and/or atmospheric pressure chemical ionization (APCI) in the positive ionisation mode unless otherwise stated.

Biotage grade silica gel was employed for column chromatographic purifications on the Biotage Isolera One Flash Chromatography system. Additionally, Analtech Uniplate preparative TLC (prep-TLC) plates (silica gel GF, 20 × 20 cm, 2000 microns) were used for prep-TLC purifications. The mobile phase solvents were AR grade and were used without further distillation. All yields reported are isolated and correspond to individual synthetic steps in a scheme.

^{1}H-NMR and ^{13}C-NMR spectra were acquired on either Bruker AV 400 (^{1}H 400.0, ^{13}C 101 MHz) or Varian Mercury 300 (^{1}H 300.1 MHz) spectrometers.

All final compounds were subjected to purity check experiments using LC-MS to ensure acceptable purity (≥95%). Melting points were measured using the Automatic Stuart Melting Point Apparatus SMP40 and are uncorrected. Purification and characterization for some selected intermediates and analogues are reported in ESI.†

6-Chloroimidazo[1,2-*b*]pyridazine (2a). Bromoacetaldehyde diethylacetal (12.0 mL, 78 mmol) was added to a suspension of 3-amino-6-chloropyridazine (**1a**) (5.00 g, 39 mmol) in absolute ethanol (99.9%) (78 mL) and deionized water (50 mL). A 48% aqueous solution of HBr (4.4 mL, 39 mmol) was added after which the suspension cleared. The reaction mixture was refluxed at 103 °C for 22 hours. The resulting brown solution was extracted with ethyl acetate (EtOAc) (100 mL × 3). The organic layers were combined after which the solvent was removed *in vacuo* to obtain **2a** as a brown solid which was used in the next step without further purification (LC-MS, ESI/APCI$^+$: m/z [M + H]$^+$ = 154.0, calculated exact mass = 153.0094, t_r = 1.5 min).

6-Chloro-3-iodoimidazo[1,2-*b*]pyridazine (3a). A reddish solution of 6-chloroimidazo[1,2-*b*]pyridazine (**2a**) (4.60 g, 30 mmol) in 30 mL of *N*,*N*-dimethylformamide (DMF) was purged with nitrogen for 30 minutes. NIS (7.41 g, 33 mmol) was added followed by the addition of another 45 mL of DMF. The reaction mixture was then left to magnetically stir at room temperature (21 °C) for 5 days (initially a suspension, the reaction mixture cleared after 2 days of stirring). DMF was then removed *in vacuo*. The resulting brown residue was taken up in 200 mL dichloromethane (DCM) and washed with deionized water (100 mL × 3), a saturated aqueous solution of a mixture of sodium metabisulfite ($Na_2S_2O_5$) and sodium bisulfite ($NaHSO_3$) (100 mL × 2). The solvent from the organic layer was removed *in vacuo* to afford **3a** as a brown solid (6.82 g, 81%); ^{1}H-NMR δ_H (300 MHz; $CDCl_3$) 7.92 (d, J = 9.4 Hz, 1H), 7.88 (s, 1H), 7.14 (d, J = 9.4 Hz, 1H); LC-MS, ESI/APCI$^+$: m/z [M + H]$^+$ = 279.8, calculated exact mass = 278.9060, t_r = 3.0 min.

General procedure for synthesis of chloro-substituted intermediates (4a–g)

A suspension of 6-chloro-3-iodoimidazo[1,2-*b*]pyridazine (**3a**) (1.0 eq.), an appropriate boronic acid or boronic acid pinacol ester (1.1 eq.), and $Pd(PPh_3)_2Cl_2$ (0.05 eq.) in DMF (3 mL mmol^{-1} of **3a**) was purged with nitrogen for 20 minutes. A 1 M aqueous solution of K_2CO_3 (1.05 eq.) was then added after which the reaction mixture was heated to 80 °C and left to magnetically stir at that temperature for 3.5–46 hours. The reaction mixture was diluted with DCM, washed with deionized water (8×), saturated aqueous solutions of $NaHCO_3$ (3×), NH_4Cl (3×) and NaCl (1×). For intermediates **4e–g**, containing the basic side chain, washing with aq NH_4Cl was avoided. After drying the organic layer ($MgSO_4$), the solvent was removed *in vacuo* and the resulting residue subjected to automated column chromatography on silica to give the chloro-substituted derivatives in 26–77% yield.

6-Chloro-3-(4-(methylsulfinyl)phenyl)imidazo[1,2-*b*]pyridazine (4a). Purified by flash chromatography (0–3% CH_3OH/DCM). Yellow solid (0.587 g, 77%); ^{1}H-NMR δ_H (300 MHz; $CDCl_3$) 8.24 (d, J = 8.2 Hz, 2H), 8.18 (s, 1H), 8.11 (d, J = 9.4 Hz, 1H), 7.82 (d, J = 8.0 Hz, 2H), 7.22 (d, J = 9.4 Hz, 1H) 2.81 (s, 3H); LC-MS, ESI/APCI$^+$: m/z [M + H]$^+$ = 292.0, calculated exact mass = 291.0233, t_r = 3.0 min.

General procedure for synthesis of diarylated imidazopyridazines (1, 4–12 and 29–32)

A suspension of the relevant chloro-substituted intermediate (**4a–g**) (1.0 eq.), appropriate boronic acid or boronic acid pinacol ester (1.1 eq.) and $Pd(PPh_3)_2Cl_2$ (0.05 eq.) in DMF (3 mL mmol^{-1} of **4a–g**) was purged with nitrogen for 20 minutes. A 1 M aqueous solution of K_2CO_3 (1.05 eq.) was then added after which the reaction mixture was heated to 100 °C and magnetically stirred at that temperature for 4–21 hours. The reaction mixture was then diluted with DCM, washed with deionized water (8×), saturated aqueous solutions of $NaHCO_3$ (3×), NH_4Cl (3×) and NaCl (1×). For analogues **6–12**, with basic side chains, washing with NH_4Cl (aq) was avoided. The organic layer was dried ($MgSO_4$ for **1** and **6–12**; Na_2SO_4 for **4**, **5** and **29–32**) after which the solvent was removed *in vacuo* and the resulting crude mixture subjected to further purification procedures.

6-(4-(Methylsulfinyl)phenyl)-3-(4-(methylsulfonyl)phenyl)-imidazo[1,2-*b*]pyridazine (4). Purified by prep-TLC (developed in 4% CH_3OH/DCM) and trituration in ethyl acetate. Yellow solid (0.0683 g, 57%), mp 236.6–239.0 °C (from ethyl acetate); R_f ($CH_3OH:CH_2Cl_2$ 4:96) 0.18; ^{1}H-NMR δ_H (400 MHz; $CDCl_3$) 8.41 (d, J = 8.8 Hz, 2H), 8.27 (s, 1H), 8.24 (d, J = 9.5 Hz, 1H), 8.19 (d, J = 8.7 Hz, 2H), 8.13 (d, J = 8.8 Hz, 2H), 7.88 (d, J = 8.7 Hz, 2H), 7.70 (d, J = 9.5 Hz, 1H), 3.15 (s, 3H), 2.84 (s, 3H); ^{13}C-NMR δ_C (101 MHz; $CDCl_3$) 151.23, 148.38, 140.09, 139.43, 137.92, 134.52, 133.74, 128.08 (3C), 127.97 (2C), 127.05 (2C), 126.65, 124.49 (2C), 116.66, 44.58, 44.00; LC-MS, APCI$^+$: m/z [M + H]$^+$ = 412.0, calculated exact mass = 411.0711, purity: 98.8%, t_r = 3.4 min.

***N*-Ethyl-*N*-(3-fluoro-4-(3-(4-(methylsulfinyl)phenyl)imidazo-[1,2-*b*]pyridazin-6-yl)benzyl)ethanamine (6).** Purified by flash chromatography (0–4% CH_3OH/DCM) and trituration in diethyl ether. Yellow solid (0.128 g, 59%), mp 110.7–113.0 °C (from diethyl ether); R_f ($CH_3OH:CH_2Cl_2$ 6 : 94) 0.32; ^{1}H-NMR δ_H (300 MHz; $CDCl_3$) 8.35 (d, J = 8.3 Hz, 2H), 8.20 (s, 1H), 8.11 (d, J = 9.0 Hz, 1H), 7.94–7.75 (m, 3H), 7.62 (d, J = 9.2 Hz, 1H), 7.46–7.34 (m, 2H), 3.76 (s, 2H), 2.81 (s, 3H), 2.70 (br s, 4H), 1.17 (t, J = 6.8 Hz, 6H); ^{13}C-NMR δ_C (100.6 MHz; $CDCl_3$) 162.1, 159.4, 148.8, 144.8, 134.1, 131.6, 130.5, 127.3 (4C), 125.8 (2C), 124.0 (3C), 119.0, 117.4, 56.6, 46.9 (2C), 44.0, 11.2 (2C); LC-MS, ESI/APCI$^+$: m/z [M + H]$^+$ = 437.1, calculated exact mass = 436.1733, purity: 99.6%, t_r = 2.4 min.

3-(3-(Methylsulfonyl)phenyl)-6-(4-(methylsulfonyl)phenyl)-imidazo[1,2-*b*]pyridazine (29). Purified by prep-TLC (developed in 4% CH_3OH/DCM). Yellow solid (0.0223 g, 20%), mp 264.0–267.5 °C (from 7% MeOH in DCM); R_f ($CH_3OH:CH_2Cl_2$ 4 : 96) 0.38; ^{1}H-NMR δ_H (400 MHz; DMSO-d$_6$) 9.12–9.08 (m, 1H), 8.56 (s, 1H), 8.53 (d, J = 8.0 Hz, 1H), 8.50 (d, J = 8.4 Hz, 2H), 8.45 (d, J = 9.6 Hz, 1H), 8.13 (d, J = 8.5 Hz, 2H), 8.09 (d, J = 9.6 Hz, 1H), 8.00–7.96 (m, 1H), 7.86 (t, J = 7.9 Hz, 1H), 3.33 (m, 6H); ^{13}C-NMR δ_C (101 MHz; DMSO-d$_6$) 150.20, 142.63, 142.04, 140.26, 140.07, 135.36, 131.32, 130.51, 129.90, 128.49 (2C), 128.17 (2C), 127.33, 126.10, 126.38, 124.60, 116.99, 44.08, 43.90; LC-MS, APCI$^+$: m/z [M + H]$^+$ = 428.0, calculated exact mass = 427.0660, purity: 95.8%, t_r = 3.5 min.

General procedure for synthesis of aminated analogues (15, 16, 18 and 21)

A suspension of 6-chloro-3-(4-(methylsulfinyl)phenyl)imidazo-[1,2-*b*]pyridazine (**4a**) (1.0 eq.), an appropriate amine (1.1 eq.), $Pd_2(dba)_3$ (0.08 eq.), XPhos (0.12 eq.) and sodium *tert*-butoxide (2.0 eq.) in anhydrous 1,4-dioxane (6.0 mL mmol^{-1} of **4a**) in a sealed tube was flashed with nitrogen for 20 minutes. The reaction mixture was then heated to 120 °C and stirred for 6–20 hours. The solvent was removed *in vacuo* after which the resulting residue was taken up in DCM, washed with saturated aqueous solutions of $NaHCO_3$ (2×) and NaCl (2×). The organic layer was dried ($MgSO_4$) (Na_2SO_4 for **16**), where after the solvent was removed *in vacuo* and obtained residue further purified.

***N*-(3-(Methylsulfinyl)phenyl)-3-(4-(methylsulfinyl)phenyl)-imidazo[1,2-*b*]pyridazin-6-amine (15).** Purified by prep-TLC (developed twice in 6% CH_3OH/DCM). Brown solid (0.0175 g, 18%); R_f ($CH_3OH:CH_2Cl_2$ 6 : 94) 0.19; ^{1}H-NMR δ_H (400 MHz; DMSO-d$_6$) 9.81 (s, 1H), 8.28 (d, J = 8.5 Hz, 2H), 8.11 (s, 1H), 8.05 (s, 1H), 8.03 (d, J = 9.7 Hz, 1H), 7.85 (d, J = 8.5 Hz, 2H), 7.77 (dd, J = 8.1, 1.3 Hz, 1H), 7.57 (t, J = 7.9 Hz, 1H), 7.31 (d, J = 7.7 Hz, 1H), 7.02 (d, J = 9.7 Hz, 1H), 2.82 (s, 3H), 2.73 (s, 3H); ^{13}C-NMR δ_C (101 MHz; DMSO-d$_6$) 151.09, 147.73, 145.44, 141.43, 138.21, 132.23, 131.62, 130.32, 127.41 (2C), 127.34 (2C), 124.69 (2C), 121.14, 117.01, 113.89, 113.50, 43.83, 43.73; LC-MS, APCI$^+$: m/z [M + H]$^+$ = 411.1, calculated exact mass = 410.0871, purity: 98.9%, t_r = 3.8 min.

3-(4-(Methylsulfinyl)phenyl)-*N*-(pyrazin-2-yl)imidazo[1,2-*b*]-pyridazin-6-amine (18). Purified by prep-TLC (developed in 5% CH_3OH/DCM). Light yellow solid (0.0242 g, 29%); R_f ($CH_3OH:CH_2Cl_2$ 6 : 94) 0.3; ^{1}H-NMR δ_H (400 MHz; DMSO-d$_6$) 10.43 (s, 1H), 9.23 (d, J = 1.3 Hz, 1H), 8.38 (dd, J = 2.6, 1.5 Hz, 1H), 8.35 (d, J = 8.5 Hz, 2H), 8.26 (d, J = 2.6 Hz, 1H), 8.16–8.09 (m, 2H), 7.83 (d, J = 8.5 Hz, 2H), 7.43 (d, J = 9.7 Hz, 1H), 2.82 (s, 3H); ^{13}C-NMR δ_C (101 MHz; DMSO-d$_6$) 150.20, 149.95, 145.70, 142.75, 138.50, 137.91, 135.82, 132.81, 131.46, 127.50, 127.35 (2C), 127.09, 124.45 (2C), 113.48, 43.68; LC-MS, APCI$^+$: m/z [M + H]$^+$ = 351.1, calculated exact mass = 350.0950, purity: 96.5%, t_r = 3.7 min.

General procedure for synthesis of diarylated imidazopyridazines 3 and 28

A suspension of 6-chloro-3-iodoimidazo[1,2-*b*]pyridazine (**3a**) (1.0 eq.), an appropriate boronic acid (2.2 eq.), and $Pd(PPh_3)_2Cl_2$ (0.10 eq.) in anhydrous DMF (2.6 mL) was purged with nitrogen for 30 minutes. A 1 M aqueous solution of K_2CO_3 (2.1 eq.) was then added. The reaction mixture was heated to 100 °C and left to magnetically stir at this temperature for 24 hours (**28**) and 15 hours (**3**). The reaction mixture was then diluted with DCM (60 mL), washed with deionized water (40 mL × 7), saturated aqueous solutions of $NaHCO_3$ (40 mL × 3), NH_4Cl (40 mL × 3), and NaCl (40 mL × 1). The organic layer was dried (Na_2SO_4), after which the solvent was removed *in vacuo*. The resulting crude mixture was subjected to prep-TLC purification to get the title compounds.

3,6-Bis(4-(methylsulfinyl)phenyl)imidazo[1,2-*b*]pyridazine (3). Purified by prep-TLC (developed twice in 5% CH_3OH/DCM). Crystallized in diethyl ether. Yellow solid (0.0665 g, 39%); mp 180.4–182.3 °C (from diethyl ether); R_f ($CH_3OH:CH_2Cl_2$ 4 : 96) 0.21; ^{1}H-NMR δ_H (400 MHz; DMSO-d$_6$) 8.48 (d, J = 8.8 Hz, 2H), 8.45 (s, 1H), 8.39 (d, J = 9.6 Hz, 1H), 8.35 (d, J = 8.7 Hz, 2H), 7.99 (d, J = 9.6 Hz, 1H), 7.91 (d, J = 8.6 Hz, 2H), 7.89 (d, J = 8.8 Hz, 2H), 2.84 (s, 3H), 2.83 (s, 3H); ^{13}C-NMR δ_C (101 MHz; DMSO-d$_6$) 151.04, 148.96, 145.89, 140.15, 137.75, 135.09, 131.10, 128.43 (2C), 127.23 (3C), 127.13, 124.91 (2C), 124.68 (2C), 116.98, 43.67 (2C); LC-MS, APCI$^+$: m/z [M + H]$^+$ = 396.1, calculated exact mass = 395.0762, purity: 98.5%, t_r = 3.7 min.

6-(3-(Methylsulfinyl)phenyl)imidazo[1,2-*b*]pyridazine (4h). A suspension of 6-chloroimidazo[1,2-*b*]pyridazine (**2a**) (1.50 g, 9.8 mmol), 3-methylsulfinylphenylboronic acid (1.78 g, 9.8 mmol), and $Pd(PPh_3)_2Cl_2$ (0.344 g, 0.49 mmol) in anhydrous DMF (30 mL) was purged with nitrogen for 30 minutes. A 1 M aqueous solution of K_2CO_3 (1.42 g, 10.29 mmol) was then added. The reaction mixture was heated to 100 °C and magnetically stirred at this temperature for 3.25 hours. The black reaction mixture was then diluted with DCM (150 mL), washed with deionized water (75 mL × 8), saturated aqueous solutions of $NaHCO_3$ (75 mL × 3), NH_4Cl (75 mL × 1) and NaCl (50 mL × 5). After drying ($MgSO_4$) the organic layer, the solvent was removed *in vacuo* and the resulting crude mixture subjected to flash column chromatography (0–5% CH_3OH/DCM) to afford the phenylated intermediate, **4h** which was further crystallized in diethyl ether to obtain a yellow solid

(1.20 g, 48%); ^{1}H-NMR δ_H (400 MHz; $CDCl_3$) 8.36 (td, *J* = 1.8, 0.6 Hz, 1H), 8.25 (d, *J* = 9.6 Hz, 1H), 8.15 (dt, *J* = 7.7, 1.7 Hz, 1H), 8.10 (d, *J* = 1.3 Hz, 1H), 7.89 (d, *J* = 1.4 Hz, 1H), 7.78 (dt, *J* = 7.8, 1.5 Hz, 1H), 7.74 (td, *J* = 7.6, 0.6 Hz, 1H), 7.69 (d, *J* = 9.5 Hz, 1H), 2.84 (s, 3H); LC-MS, ESI$^+$: *m/z* [M + H]$^+$ = 258.1, calculated exact mass = 257.0623, t_r = 3.1 min.

3-Bromo-6-(3-(methylsulfinyl)phenyl)imidazo[1,2-*b*]-pyridazine (4i). A brown solution of 6-(3-(methylsulfinyl)-phenyl)imidazo[1,2-*b*]pyridazine (**4h**) (1.20 g, 4.7 mmol) in anhydrous DMF (4 mL) was purged with nitrogen for 30 minutes. NBS (0.912 g, 5.1 mmol) was added where after the reaction mixture was stirred at room temperature (23 °C) for 22 hours. The reaction mixture, containing a yellow precipitate at this point, was taken up in 100 mL DCM and washed with deionized water (75 mL × 8), saturated aqueous solutions of $NaHCO_3$ (75 mL × 2), NH_4Cl (75 mL × 2) and NaCl (75 mL × 1). The organic layer was dried ($MgSO_4$) after which the solvent was removed *in vacuo*. The obtained oily residue was crystallized and triturated with ethyl acetate for 30 minutes. The solid was filtered and washed with ethyl acetate to give **4i** as a yellow solid (0.939 g, 59%); ^{1}H-NMR δ_H (300 MHz; $CDCl_3$) 8.44–8.35 (m, 2H), 8.29–8.23 (m, 1H), 7.93 (s, 1H), 7.90–7.73 (m, 3H), 2.85 (s, 3H); LC-MS, ESI$^+$: *m/z* [M + H]$^+$ = 336.0 & 338.0, calculated exact mass = 334.9728, t_r = 3.9 min.

3,6-Bis(3-(methylsulfinyl)phenyl)imidazo[1,2-*b*]pyridazine (13). A suspension of 3-bromo-6-(3-(methylsulfinyl)phenyl)-imidazo[1,2-*b*]pyridazine (**4i**) (0.100 g, 0.30 mmol), 3-methylsulfinylphenylboronic acid (0.0602 g, 0.33 mmol), and $Pd(PPh_3)_2Cl_2$ (0.0105 g, 0.015 mmol) in anhydrous DMF (2.0 mL) was purged with nitrogen for 30 minutes. A 1 M aqueous solution of K_2CO_3 (0.0435 g, 0.32 mmol) was then added. The reaction mixture was heated to 100 °C and magnetically stirred at this temperature for 20 hours. The reaction mixture was then diluted with DCM (60 mL), washed with deionized water (40 mL × 6), saturated aqueous solutions of $NaHCO_3$ (40 mL × 3), NH_4Cl (40 mL × 3) and NaCl (40 mL × 1). The organic layer was dried ($MgSO_4$), where after the solvent was removed *in vacuo*. The resulting crude mixture was subjected to prep-TLC (developed twice in 4% CH_3OH/DCM) to get **13** as an oil. Crystallization with diethyl ether gave **13** as a yellow solid (0.0481 g, 40%); R_f ($CH_3OH:CH_2Cl_2$ 4:96) 0.17; ^{1}H-NMR δ_H (400 MHz; DMSO-d_6) 8.80 (m, 1H), 8.48–8.42 (m, 2H), 8.42–8.35 (m, 2H), 8.33 (dt, *J* = 7.6, 1.6 Hz, 1H), 8.03 (d, *J* = 9.5 Hz, 1H), 7.94–7.88 (m, 1H), 7.82 (t, *J* = 7.7 Hz, 1H), 7.76 (t, *J* = 7.7 Hz, 1H), 7.73–7.69 (m, 1H), 2.88 (s, 3H), 2.86 (s, 3H) ^{13}C-NMR δ_C (101 MHz; DMSO-d_6) 150.75, 148.34, 147.67, 140.06, 136.44, 134.81, 130.65, 130.14, 129.89, 129.73, 128.72, 127.15, 127.08, 125.63, 123.28, 122.60, 121.19, 116.75, 43.97, 43.82; LC-MS, APCI$^+$: *m/z* [M + H]$^+$ = 396.1, calculated exact mass = 395.0762, purity: 99.8%, t_r = 3.8 min.

General procedure for synthesis of aminated analogues (24–27)

A suspension of 3-bromo-6-(3-(methylsulfinyl)phenyl)imidazo-[1,2-*b*]pyridazine (**4i**) (1.0 eq.), an appropriate amine (1.3 eq.), $Pd_2(dba)_3$ (0.2 eq.), BrettPhos (0.12 eq.) and Cs_2CO_3 (2.0 eq.) in anhydrous 1,4-dioxane (2 mL) in a sealed tube was flashed with nitrogen for 20 minutes. The reaction mixture was then heated to 120 °C and stirred for 5–39 hours. The solvent was removed *in vacuo* after which the resulting black residue was taken up in DCM (60 mL), washed with saturated aqueous solutions of $NaHCO_3$ (40 mL × 3) and NaCl (40 mL × 1). The organic layer was dried (Na_2SO_4), after which the solvent was removed *in vacuo* and the crude mixture further purified.

6-(3-(Methylsulfinyl)phenyl)-*N*-(4-(methylsulfonyl)phenyl)-imidazo[1,2-*b*]pyridazin-3-amine (24). Purified by prep-TLC (developed thrice in 2.5% CH_3OH/DCM). Crystallized in diethyl ether. Brown solid (0.0121 g, 9%); mp 105.0–107.2 °C (from diethyl ether); R_f ($CH_3OH:CH_2Cl_2$ 4:96) 0.23; ^{1}H-NMR δ_H (400 MHz; DMSO-d_6) 9.13 (s, 1H), 8.32–8.25 (m, 2H), 8.18 (d, *J* = 7.7 Hz, 1H), 7.91–7.80 (m, 3H), 7.78–7.68 (m, 3H), 6.99 (d, *J* = 8.4 Hz, 2H), 3.11 (s, 3H), 2.80 (s, 3H); ^{13}C-NMR δ_C (101 MHz; DMSO-d_6) 150.57, 149.91, 148.01, 136.65, 135.99, 130.46, 130.33, 129.64, 129.31 (2C), 127.66, 127.04, 126.95, 125.62, 122.61, 115.86, 114.13 (2C), 44.75, 43.63; LC-MS, APCI$^+$: *m/z* [M + H]$^+$ = 427.1, calculated exact mass = 426.0820, purity: 97.7%, t_r = 3.4 min.

Conflicts of interest

There are no conflicts to declare.

Acknowledgements

We gratefully acknowledge the support of the University of Cape Town, South African Medical Research Council and the South African Research Chairs Initiative of the Department of Science and Technology administered through the South African National Research Foundation (K.C.). At Swiss TPH, we thank Christoph Fischli, Christin Gumpp, Sibylle Sax and Christian Scheurer for assistance in performing the antimalarial assays.

Notes and references

1 World Health Organization, *World Malaria Report*, 2017.

2 N. J. White, Antimalarial Drug Resistance, *J. Clin. Invest.*, 2004, **113**, 1084–1092.

3 C. H. Sibley, J. E. Hyde, P. F. Sims, C. V. Plowe, J. G. Kublin, E. K. Mberu, A. F. Cowman, P. A. Winstanley, W. M. Watkins and A. M. Nzila, Pyrimethamine–sulfadoxine Resistance in Plasmodium Falciparum: What Next?, *Trends Parasitol.*, 2001, **17**, 570–571.

4 D. J. Terlouw, B. L. Nahlen, J. M. Courval, S. K. Kariuki, O. S. Rosenberg, A. J. Oloo, M. S. Kolczak, W. A. Hawley, A. A. Lal and F. O. T. Kuile, Sulfadoxine-Pyrimethamine in Treatment of Malaria in Western Kenya: Increasing Resistance and Underdosing, *Antimicrob. Agents Chemother.*, 2003, **47**, 2929–2932.

5 D. C. Warhurst, Resistance to Antifolates in Plasmodium Falciparum, the Causative Agent of Tropical Malaria, *Sci. Prog.*, 2002, **85**, 89–111.

6 K.-I. Kusakabe, H. Yoshida, K. Nozu, H. Hashizume, G. Tadano, J. Sato, Y. Tamura and Y. Mitsuoka, Imidazo[1,2-b] Pyridazine and Pyrazolo[1,5-a]Pyrimidine Derivatives and Their Use as Protein Kinase Inhibitors, WO2011/013729A1, 2011.

7 Y. Xu, B. G. Brenning, S. G. Kultgen, X. Liu, M. Saunders and K.-K. Ho, Preparation of Imidazo[1,2-b]Pyridazine and Pyrazolo[1,5-a]Pyrimidine Derivatives as Protein Kinase Inhibitors, US20120058997, 2012.

8 D. B. Moran, D. W. Powell and J. D. Albright, Imidazo[1,2-b] Pyridazines, US4569934A, 1986.

9 S. Matsumoto, N. Miyamoto, T. Hirayama, H. Oki, K. Okada, M. Tawada, H. Iwata, K. Nakamura, S. Yamasaki, H. Miki, A. Hori and S. Imamura, Structure-Based Design, Synthesis, and Evaluation of Imidazo[1,2-b]Pyridazine and Imidazo[1,2-a]Pyridine Derivatives as Novel Dual c-Met and VEGFR2 Kinase Inhibitors, *Bioorg. Med. Chem.*, 2013, **21**, 7686–7698.

10 S. Osborne, T. Chapman, J. Large, N. Bouloc and C. Wallace, Fused Heterocyclic Compounds for Use in the Treatment of Malaria, WO2011101640, 2011.

11 G. Lemercier, A. Fernandez-Montalvan, J. P. Shaw, D. Kugelstadt, J. Bomke, M. Domostoj, M. K. Schwarz, A. Scheer, B. Kappes and D. Leroy, Identification and Characterization of Novel Small Molecules as Potent Inhibitors of the Plasmodial Calcium-Dependent Protein Kinase 1, *Biochemistry*, 2009, **48**, 6379–6389.

12 N. K. Sahu and D. V. Kohli, Structural Insight for Imidazopyridazines as Malarial Kinase PfPK7 Inhibitors Using QSAR Techniques, *Med. Chem.*, 2012, **8**, 636–648.

13 C. W. McNamara, M. C. S. Lee, C. S. Lim, S. H. Lim, J. Roland, A. Nagle, O. Simon, B. K. S. Yeung, A. K. Chatterjee, S. L. McCormack, M. J. Manary, A.-M. Zeeman, K. J. Dechering, T. R. S. Kumar, P. P. Henrich, K. Gagaring, M. Ibanez, N. Kato, K. L. Kuhen, C. Fischli, M. Rottmann, D. M. Plouffe, B. Bursulaya, S. Meister, L. Rameh, J. Trappe, D. Haasen, M. Timmerman, R. W. Sauerwein, R. Suwanarusk, B. Russell, L. Renia, F. Nosten, D. C. Tully, C. H. M. Kocken, R. J. Glynne, C. Bodenreider, D. A. Fidock, T. T. Diagana and E. A. Winzeler, Targeting Plasmodium PI(4)K to Eliminate Malaria, *Nature*, 2013, **504**, 248–253.

14 C. Le Manach, D. Gonzàlez Cabrera, F. Douelle, A. T. Nchinda, Y. Younis, D. Taylor, L. Wiesner, K. L. White, E. Ryan, C. March, S. Duffy, V. M. Avery, D. Waterson, M. J. Witty, S. Wittlin, S. A. Charman, L. J. Street and K. Chibale, Medicinal Chemistry Optimization of Antiplasmodial Imidazopyridazine Hits from High Throughput Screening of a SoftFocus Kinase Library: Part 1, *J. Med. Chem.*, 2014, **57**, 2789–2798.

15 C. Le Manach, T. Paquet, D. Gonzàlez Cabrera, Y. Younis, D. Taylor, L. Wiesner, N. Lawrence, S. Schwager, D. Waterson, M. J. Witty, S. Wittlin, L. J. Street and K. Chibale, Medicinal Chemistry Optimization of Antiplasmodial Imidazopyridazine Hits from High Throughput Screening of a SoftFocus Kinase Library: Part 2, *J. Med. Chem.*, 2014, **57**, 8839–8848.

16 C. Le Manach, T. Paquet, C. Brunschwig, M. Njoroge, Z. Han, D. Gonzàlez Cabrera, S. Bashyam, R. Dhinakaran, D. Taylor, J. Reader, M. Botha, A. Churchyard, S. Lauterbach, T. L. Coetzer, L.-M. Birkholtz, S. Meister, E. A. Winzeler, D. Waterson, M. J. Witty, S. Wittlin, M.-B. Jiménez-Díaz, M. Santos Martínez, S. Ferrer, I. Angulo-Barturen, L. J. Street and K. Chibale, A Novel Pyrazolopyridine with in Vivo Activity in Plasmodium Berghei - and Plasmodium Falciparum - Infected Mouse Models from Structure–Activity Relationship Studies around the Core of Recently Identified Antimalarial Imidazopyridazines, *J. Med. Chem.*, 2015, **58**, 8713–8722.

17 L. Du, M. Li and Q. You, The Interactions Between HERG Potassium Channel and Blockers, *Curr. Top. Med. Chem.*, 2009, **9**, 330–338.

18 C. Jamieson, E. M. Moir, Z. Rankovic and G. Wishart, Medicinal Chemistry of HERG Optimizations: Highlights and Hang-Ups, *J. Med. Chem.*, 2006, **49**, 5029–5046.

19 L. Zhang, H. Zhu, A. Mathiowetz and H. Gao, Deep Understanding of Structure–solubility Relationship for a Diverse Set of Organic Compounds Using Matched Molecular Pairs, *Bioorg. Med. Chem.*, 2011, **19**, 5763–5770.

20 A. G. Leach, H. D. Jones, D. A. Cosgrove, P. W. Kenny, L. Ruston, P. MacFaul, J. M. Wood, N. Colclough and B. Law, Matched Molecular Pairs as a Guide in the Optimization of Pharmaceutical Properties; a Study of Aqueous Solubility, Plasma Protein Binding and Oral Exposure, *J. Med. Chem.*, 2006, **49**, 6672–6682.

21 S. Forster, G. Buckton and A. E. Beezer, The Importance of Chain Length on the Wettability and Solubility of Organic Homologs, *Int. J. Pharm.*, 1991, **72**, 29–34.

22 J. P. Wolfe, S. Wagaw and S. L. Buchwald, An Improved Catalyst System for Aromatic Carbon–Nitrogen Bond Formation: The Possible Involvement of Bis(Phosphine) Palladium Complexes as Key Intermediates, *J. Am. Chem. Soc.*, 1996, **118**, 7215–7216.

23 M. S. Driver and J. F. Hartwig, A Second-Generation Catalyst for Aryl Halide Amination: Mixed Secondary Amines from Aryl Halides and Primary Amines Catalyzed by (DPPF)PdCl2, *J. Am. Chem. Soc.*, 1996, **118**, 7217–7218.

24 M. Ishikawa and Y. Hashimoto, Improvement in Aqueous Solubility in Small Molecule Drug Discovery Programs by Disruption of Molecular Planarity and Symmetry, *J. Med. Chem.*, 2011, **54**, 1539–1554.